Eur Radiol (2007) 17: 2112–2125
DOI 10.1007/s00330-006-0575-9

Alexandra Borges
Jan Casselman

Imaging the cranial nerves: Part I: Methodology, infectious and inflammatory, traumatic and congenital lesions

Received: 12 July 2006
Revised: 13 November 2006
Accepted: 28 December 2006
Published online: 24 February 2007

A. Borges (✉)
Department of Radiology,
Instituto Português de Oncologia
Francisco Gentil- Centro de Lisboa,
Rua Professor Lima Basto,
1093 Lisboa Codex, Portugal
e-mail: borgesalexandra@clix.pt
Tel.: +351-21-3660812
Fax: +351-21-3660813

J. Casselman
Department of Radiology,
A.Z. St. Jan Brugge Hospital,
Brugge, Belgium

J. Casselman
Department of Radiology,
A.Z. St. Augustinus
Antwerpen Hospitals,
Antwerpen, Belgium

Abstract Many disease processes manifest either primarily or secondarily by cranial nerve deficits. Neurologists, ENT surgeons, ophthalmologists and maxillo-facial surgeons are often confronted with patients with symptoms and signs of cranial nerve dysfunction. Seeking the cause of this dysfunction is a common indication for imaging. In recent decades we have witnessed an unprecedented improvement in imaging techniques, allowing direct visualization of increasingly small anatomic structures. The emergence of volumetric CT scanners, higher field MR scanners in clinical practice and higher resolution MR sequences has made a tremendous contribution to the development of cranial nerve imaging. The use of surface coils and parallel imaging allows sub-millimetric visualization of nerve branches and volumetric 3D imaging. Both with CT and MR, multiplanar and curved reconstructions can follow the entire course of a cranial nerve or branch, improving tremendously our diagnostic yield of neural pathology. This review article will focus on the contribution of current imaging techniques in the depiction of normal anatomy and on infectious and inflammatory, traumatic and congenital pathology affecting the cranial nerves. A detailed discussion of individual cranial nerves lesions is beyond the scope of this article.

Keywords Cranial nerves · High-resolution CT · High-resolution MRI · Cranial neuropathy · Cranial neuralgia

Introduction

Cranial nerves are responsible for much of our pleasure through the senses of vision, hearing, smell and taste and for non-verbal communication of our emotions through facial expression, which defines us as unique individuals.

There are 12 cranial nerves exiting the central nervous system from cephalad to caudad. With the exception of cranial nerves I and II, the remainder exit the brain stem from the ponto-mesencephalic junction to the medulla oblongata, travel through the perimesencephalic and basal cisterns, and exit the intracranial compartment through the neurovascular foramina of the skull base from anterior to posterior. Cranial nerve IV is unique in that it is the only cranial nerve that exits the brain stem dorsally and gives complete crossed enervation, whereas cranial nerve VI is the single cranial nerve with an ascending course before exiting the intracranial compartment [1–4].

Cranial nerve X is the longest of the cranial nerves, traveling from the posterior skull base to the abdominal viscera; the trigeminal nerve is the largest and the most widely distributed in the supra-hyoid neck, and the facial nerve is the most commonly paralyzed nerve of the human body [1, 4–6].

Disease processes that affect the cranial nerves span a wide gamut and include both primary and secondary pathologic conditions. It is not uncommon that cranial nerve dysfunction is the first sign of neighboring disease due to compression, perineural spread or metastases. Therefore, neurologists, ENT surgeons, ophthalmologists and maxillo-facial surgeons are often confronted with cranial nerve deficits when they first examine a patient, and

cranial nerve dysfunction is a common indication for imaging [5–7].

In the last decades we have witnessed an unprecedented improvement in imaging techniques, allowing direct visualization of increasingly small anatomic structures. The wider use of volumetric CT scanners, higher field MR scanners in clinical practice and higher resolution MR sequences has made a tremendous contribution to the development of cranial nerve imaging. Parallel imaging in combination with small surface coils is now able to depict sub-millimetric nerve branches, and volumetric 3D imaging, both with CT and MR, provides multiplanar and curved reconstruction planes that can follow the entire course of a cranial nerve or branch improving tremendously our diagnostic yield of neural pathology [6, 8–10] (Fig. 1a to d). Henceforth, an increasing demand on knowledge of cranial nerve anatomy and function is placed upon radiologists in order to be able to adequately tailor imaging studies. As MR imaging becomes more sophisticated and more dedicated, high-resolution studies with smaller fields of view are required; it becomes mandatory to limit the examination to the presumptive anatomic area of interest to keep the study within a reasonable time frame. In order to achieve this goal, radiologists need detailed clinical and neurological information. As it is not unusual that head and neck radiologists and neuroradiologists are the first specialists patients are referred to, a radiology consultation including a concise clinical history and neurological exam should be undertaken whenever adequate information is not provided by the referring clinician.

Imaging

Although the larger cranial nerves such as the optic and trigeminal nerves and the VII-VIIIth nerve complex are often visualized on routine CT and MR imaging studies of the brain, smaller cranial nerves and nerve branches are only visible when the appropriate technique is used.

CT and MR have a complimentary role in the evaluation of cranial nerve pathology, and together offer a full picture of bone and soft tissue changes. However, MR is the method of choice and, in most instances, is the only modality needed to provide all of the necessary information. Angiography is no longer used routinely as a diagnostic tool, but may be required for preoperative embolization of highly vascular tumors to exclude additional small glomus lesions and to exclude dural fistulas in cases of tinnitus when MR and CT are negative and patients have severe complaints. The role of ultrasound is limited to the evaluation of infrahyoid cervical masses, namely to guide fine-needle aspiration biopsies.

CT is particularly well suited to depicting neurovascular skull base foramina and canals and is used to provide a roadmap of the skull base and facial bone anatomy preoperatively. The effect of a lesion upon the adjacent bone is a useful tool in differentiating aggressive, rapidly growing processes from benign and indolent lesions. Whereas the former are associated with a permeative or a "moth-eaten" pattern, the latter tend to expand and remodel adjacent bone [3, 11, 12]. Intravenous administration of iodinated contrast increases the study sensitivity, determines the relationship between lesions and adjacent vascular structures and is mandatory to depict neurovascular conflicts. Volumetric acquisition achieved with 16, 32, 40 or 64 multidetector CT scanners and adequate post-processing software can depict most cranial nerves and adjacent vascular branches. One millimeter and sub-millimeter CT images can be reconstructed in several planes. Preferably, studies should be viewed and post-processed in dedicated workstations to minimize film overload. Minimal requirements for adequate CT imaging of skull base and facial neurovascular foramina include 3-mm-thick slices without interslice gap in at least two orthogonal planes, obtained both in soft tissue and high-resolution bone algorithms (Table 1) [5, 13]. However, most scanners are now able to acquire images of 1.25-mm thickness and 1-mm computer reconstructions. Studies should include the entire course of the affected cranial nerve from its brain-stem nuclei to its peripheral branches when a clinical topographic diagnosis cannot be achieved [5].

MR imaging studies are more time consuming and more susceptible to motion artifacts. Therefore, topognostic testing is of utmost importance in the study design, increasing significantly the diagnostic yield while decreasing the examination time. High-field scanners of 1-T or above provide a better signal-to-noise ratio, while steeper gradients give better spatial resolution and decrease the examination time. Nuclear and supranuclear lesions are studied using a regular MR protocol of the brain and upper cervical spinal cord, including T1W images pre- and post-gadolinium, fast spin echo (FSE) T2W images and diffusion-weighted imaging (DWI). For the cisternal segments of cranial nerves, 3DFT heavily T2W sequences (CISS, DRIVE or FIESTA) are particularly well suited, depicting the nerve as a linear hypointense structure surrounded by hyperintense CSF within adjacent cisterns [5, 6, 9, 10, 13] (Figs. 1b and c). These sequences provide very good CSF-nerve contrast and very thin submillimeter slices (0.7 mm every 0.35 mm), allowing for 3D reconstructions and virtual endoscopic views (Fig. 1a). High-resolution 3DFT TOF MRA (3D FISP or FLASH) and/or contrast-enhanced MRA, with careful analysis of MIP (maximum intensity projection) multiplanar reconstructions and source images, is the method of choice to depict neurovascular conflicts [5, 6, 14, 15]. These sequences depict the vessels as hyperintense structures within the hypointense CSF and nerves as linear structures of intermediate signal intensity, isointense to brain parenchyma. Exquisite anatomic depiction of the remaining segments is provided by high-resolution 3DFT T1W

sequences, using a 512×512 matrix (SPGR, GRASS, MPRAGE) (Fig. 1d) pre- and fat-suppressed post-gadolinium images [5, 6]. Intravenous injection of gadolinium is mandatory to visualize cranial nerves in the parasellar or cavernous sinus region where, in normal circumstances, they are depicted as hypointense structures within the

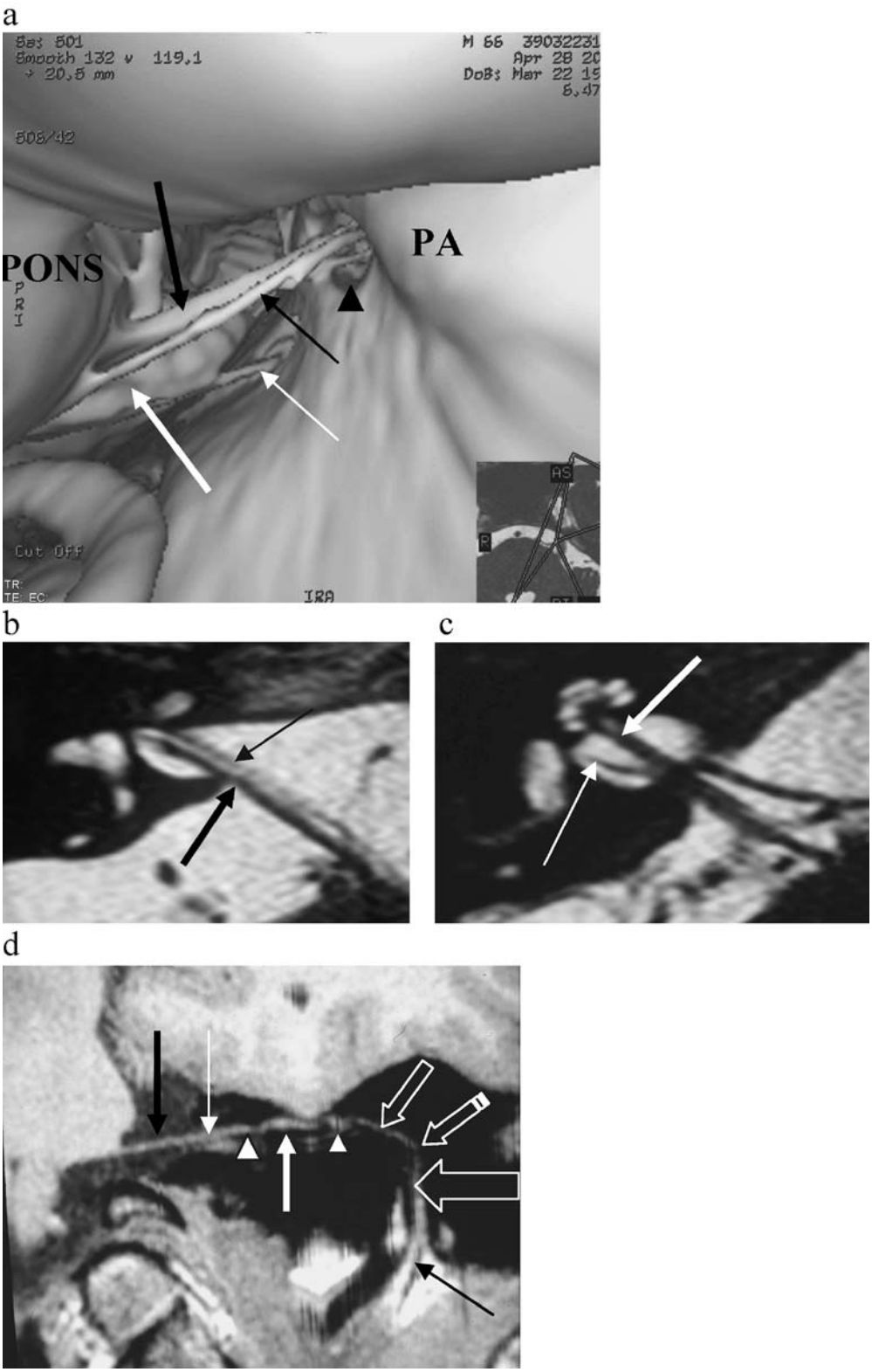

Fig. 1 **a** Tridimensional navigation reconstruction from a balanced fast field echo sequence shows the pons on the left side and the petrous apex on the right side of the image. The facial nerve is seen crossing the CPA cistern (thin black arrow) and, immediately underneath, the vestibulo-cochlear nerve (thick black arrow). These nerves enter the porus acousticus (black arrowhead) where the vestibulo-cochlear nerve divides into anterior cochlear and posterior vestibular branches. The cerebellar flocculus is seen immediately below (thick white arrow). More inferiorly, crossing the peri-bulbar cistern, are the lower cranial nerves IX to XI entering the jugular foramen (thin white arrow). **b** and **c** Axial 3DFT CISS images through the IAC from the superior to inferior show cranial nerves VII and VIII as linear hypointense structures within the hyperintense CSF, traveling through the CPA cistern and IAC. **a** This axial section through the roof of the IAC shows the intracanalicular segment of the facial nerve anteriorly (thin black arrow) and the superior vestibular nerve posteriorly (thick black arrow) in its typical parallel configuration. **b** This axial section through the floor of the IAC shows the cochlear nerve anteriorly (thick white arrow) and the inferior vestibular nerve posteriorly (thin white arrow). **d** 3DFT MPRAGE curved reconstruction of the facial nerve shows the cisternal segment (black arrow), the intracanalicular segment (thin white arrow), the labyrinthine segment (thick white arrow) and meatus (thick white arrowhead), the geniculate ganglion (thin white arrowhead), the tympanic segment (thin hollow arrow), the posterior genu (stripped hollow arrow) and the mastoid segment (thick hollow arrow), exiting the temporal bone through the stylomastoid foramen (thin black arrow)

Table 1 CT imaging parameters for the evaluation of skull-base neurovascular foramina

CT protocol	Single slice	Multislice
Acq. plane	Axial and cor	Axial
Matrix	512×512	512×512
Collimation	1 mm	2×0.5 mm
Table feed rot	0.8 mm	0.8 mm
Reconstruction increment	1 mm	0.5 mm
Slice thickness	<3 mm	<3 mm
High-resolution algorithm	Bone and soft tissue	Bone and soft tissue
Reformation	Sagittal	Coronal and sagittal

enhancing cavernous sinus [5, 6]. SENSE (sensitive-encoding) parallel imaging using two or more phased array coils nicely depicts small peripheral nerve branches (Table 2) [6]. However, high resolution alone is not enough. It is crucial to adapt slice orientation to the course of the nerve and sequences used to the natural contrast with surrounding structures obliging the radiologist to have a detailed knowledge of cranial nerve anatomy. Therefore, MR protocols may vary from one nerve to the other.

Gadolinium injection is used to depict disruption of the blood-nerve barrier, as contrast enhancement may be the only imaging finding in infectious/inflammatory conditions, in cases of perineural spread and in small cranial nerve tumors [16].

Most pathologic processes afflicting cranial nerves manifest on imaging as abnormal enlargement and/or enhancement of the nerve, obliteration of neural-foramina fat pads, foraminal enlargement or destruction and by indirect signs of deinnervation atrophy [3, 5, 11].

Pathology

Cranial nerves can be affected by a wide variety of pathologic processes all the way along their course from the CNS to the end organ(s). For a systematic approach, it is useful to subdivide cranial nerve pathology into supra- and infranuclear and primary/intrinsic or secondary/extrinsic disease. A detailed discussion of individual cranial nerve pathology is beyond the scope of this article.

Any *supratentorial* or *brain-stem* lesion along the supranuclear or nuclear components of cranial nerves can present with cranial nerve dysfunction (Table 3). With the exception of very discrete lesions, neurological deficits are often multiple, and a careful neurological examination is

Table 2 MR imaging sequences and parameters used in the evaluation of cranial nerves

Sequence	FSE T1W[a] (+gd)	TSE T2W	3DFT MPRAGE[a] (+gd)	3DFT CISS[a]	3DFT-FISP turbo-MRA[a]
TR	684	4,000	11.6	12.25	35
TE	20	99	4.9	5.9	6.4
FA	90°	180°	12°	70°	15°
Acq. time	5 min 31 s	3 min	10 min 51 s	7 min 14 s	4 min 8 s
Thickness	2 mm	4 mm	1 mm	0.7 mm	0.75
Matrix	160×256	242×512	192×256	192×256	320×512
FOV	230	300	240	95	200
Pixel size	0.90×0.90	0.62×0.59	0.94×0.94	0.49×0.37	0.94×0.39
Weighting	T1	T2	T1	T2	T1

[a]Other similar sequences that may be used include:
FFE T1W, fast field echo T1W
2D FLASH GE, bi-dimensional fast low-angle shot gradient echo T1WI
3D-GRASS, three-dimensional gradient recalled acquisition in the steady state
3D-CE-FAST, three-dimensional contrast-enhanced Fourrier acquired steady state
3DFT-FLASH MRA, three-dimensional Fourrier transform fast low-angle shot MRA
SE, spin echo
FSE, fast spin echo
3DFT-MPRAGE, three-dimensional Fourrier transform magnetization prepared rapid gradient echo
3DFT-CISS, three-dimensional Fourrier transform constructive interference in the steady state
3DFT-FISP MRA, three-dimensional Fourrier transform fast-in-flow steady-state precession

Table 3 Cranial nerve pathology

Pathology	
(1) Supranuclear (central)	
Vascular lesions	Infarct (ischemic or hemorrhagic), vascular malformation
Demyelinating disease	Multiple sclerosis
Neoplasm	Primary and secondary, intra- or extra-axial
Infection/inflammation	Parenchymal, meningeal
Trauma	
(2) Infranuclear (peripheral)	
Infectious	Viral, bacterial, fungal and parasitic infection
Post-infectious	Bell's palsy, Ramsay-Hunt syndrome (herpes zoster cephalicus), ophthalmoplegic migraine, Guillain-Barré and Miller-Fisher syndromes
Inflammatory	Sarcoidosis, Wegener's granulomatosis, vasculitis, Tolosa-Hunt syndrome
Neoplastic	Primary: nerve sheath tumors (schwannoma, neurofibroma), hemangioma and other vascular neoplasms, paraganglioma, choristoma
	Secondary: direct invasion, hematogenous metastases or perineural spread of carcinoma, lymphoma, leukemia
Physical or chemical trauma	Direct or indirect trauma, radiation, neurotoxic drugs
Congenital	Otoskeletal, otocranial-facial and otocervical syndromes (Mobius syndrome, Goldenhar-Gorlin, etc.)

frequently able to pinpoint the lesion to a particular area (Figs. 2 and 3) (for example, a patient presenting with deficits of cranial nerves VI and VII will likely have a lesion in the dorsal brain stem at the floor of the IVth ventricle where the nucleus of cranial nerve VI and the fascicular fibers of the facial nerve lay together) (Fig. 2).

Infranuclear cranial neuropathies are grouped into broad categories of disease that include infectious and inflammatory conditions, trauma, benign and malignant neoplasms, and vascular, metabolic, degenerative and congenital disease. Cranial nerves may also be secondarily involved by direct compression or invasion from neighboring lesions or from perineural spread of extrinsic disease (Table 3) [5, 16]. This article will focus on infectious and inflammatory, traumatic and congenital cranial neuropathies.

1. Infectious and inflammatory
   The most common infectious/inflammatory conditions affecting cranial nerves are viral neuronitis secondary to herpes simplex, varicella zoster, cytomegalovirus or

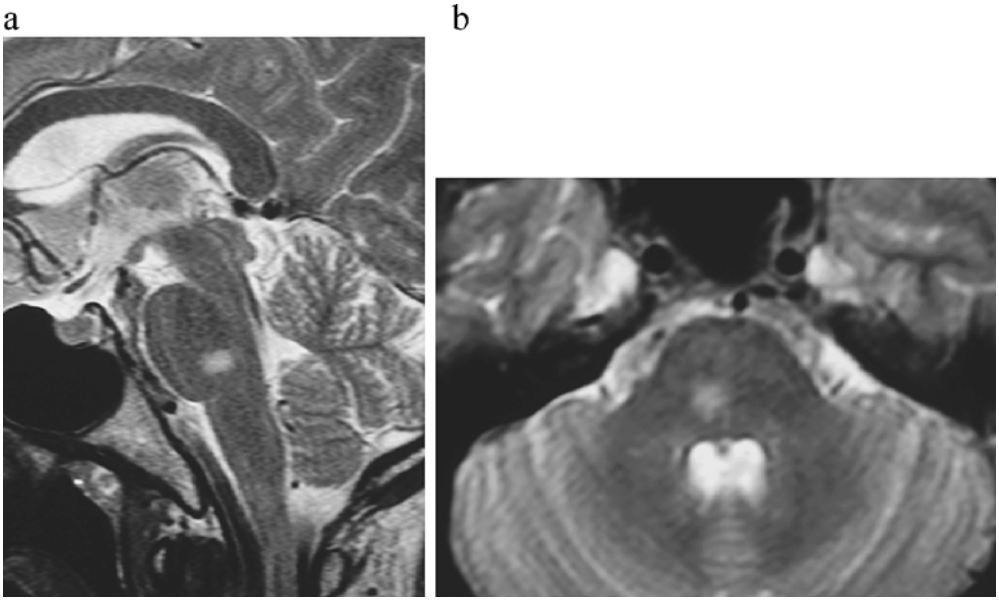

Fig. 2 Demyelinating plaque in multiple sclerosis. **a** Sagittal and (**b**) axial FSE T2W images through the brain stem showing a discrete, hyperintense, ill-defined lesion at the dorso-lateral aspect of the pons at the expected location of the mesencephalic nucleus of the trigeminal nerve. This was the inaugural lesion in this patient with multiple sclerosis

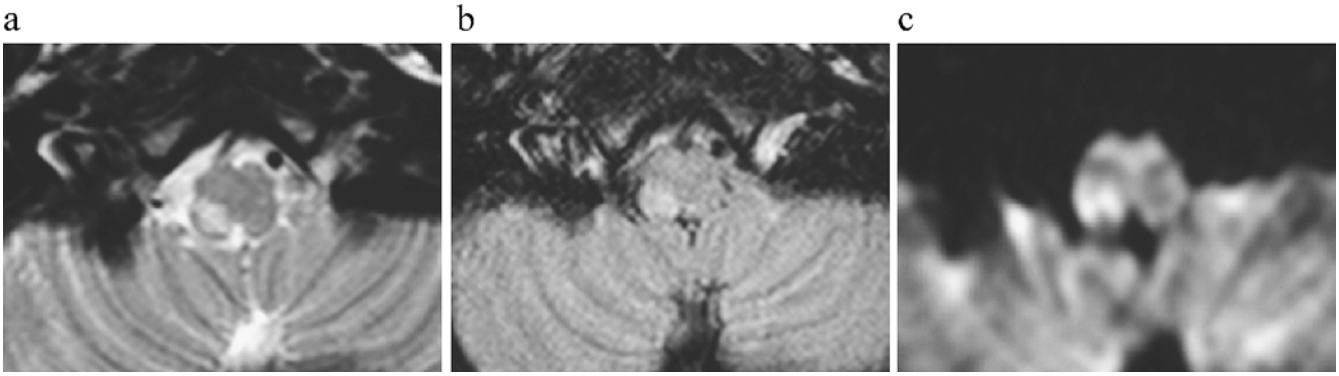

Fig. 3 Acute ischemic infarct in the territory of the posterior and inferior cerebellar artery (PICA). **a** Axial FSE T2W, (**b**) FLAIR and (**c**) DWI (b1000) show a discrete, hyperintense lesion at the dorsolateral aspect of the bulbo-medullary junction, affecting the nuclei of the lower cranial nerves, in a patient presenting with an incomplete Wallenberg syndrome (acute infarction in the posterior-inferior cerebellar artery territory)

human immunodeficiency virus (HIV) infection [5, 11]. The facial nerve is the most commonly affected by viral neuronitis, a condition known as Bell's palsy, thought to result from reactivation of a dormant herpes virus lodged in the geniculate ganglion (Fig. 4). Second in frequency is a herpes zoster infection that tends to affect the facial and vestibulocochlear nerves, but seldom the trigeminal nerve [5, 11, 17], called herpes zoster oticus, herpes zoster cephalicus or Ramsay-Hunt syndrome [5, 11, 17, 18] (Fig. 5).

Bacterial infection is much less frequent and is usually secondary to adjacent infectious processes left untreated. It was a common occurrence in the pre-antibiotic era, but is currently seldom seen with the exception of immunocompromised and neglected patients. The primary infectious focus is often the middle ear cavity or paranasal sinuses with secondary spread of infection into the petrous apex and skull base leading to petrous apicitis and osteomyelitis (Fig. 6) [3, 5, 11, 12, 19]. Cranial nerves most commonly affected are, in decreasing order of frequency, the facial nerve in its intratemporal segments, the trigeminal nerve and oculomotor nerves within the cavernous sinus, the lower cranial nerves at the jugular foramen and the optic nerve at the orbital apex. Clinically, patients manifest with various syndromes: petrous apex/Gradenigo's, cavernous sinus, jugular foramen/Vernet's and orbital apex/Tolosa-Hunt syndromes, respectively [20]. Necrotizing or malignant otitis externa, a *Pseudomonas aeruginosa* infection afflicting predominantly diabetic patients, is associated with the highest rate of facial nerve involvement, an ominous prognostic sign [5, 11, 12].

Lyme's disease, a spirochetal infection caused by *Borrellia burgdorferi*, courses with facial nerve palsy in 10% of cases, among which 25% are bilateral. Cranial neuritis associated with this disease may affect cranial nerves III to VIII [5, 16]. Infectious/inflammatory meningitis with a propensity to the basilar cisterns often develops with cranial nerve deficits and includes tuberculous, fungal, parasitic and non-infectious granulomatoses such as sarcoidosis [3, 5, 16, 21]. Inflammatory material is deposited within the cerebello-pontine angle (CPA), perimesencephalic and basilar cisterns encasing the cisternal segments of

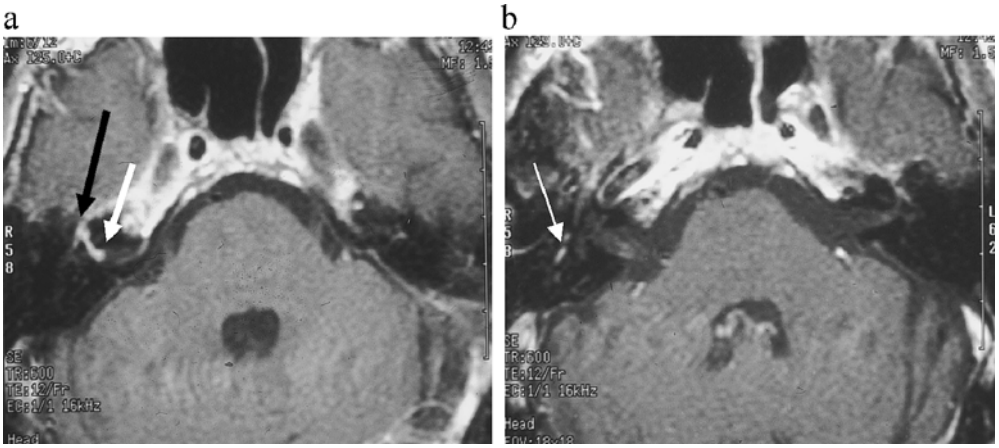

Fig. 4 Bell's palsy (HSV neuronitis). Axial post-gadolinium T1W images through the temporal bone. **a** Shows intense, smooth and homogeneous contrast enhancement along the labyrinthine and meatal (white arrow) segments of the right facial nerve as well as in the geniculate ganglion (black arrow). **b** Also note enhancement along the tympanic segment of the facial nerve (thin white arrow). This patient presented with acute facial nerve paralysis (Bell's palsy)

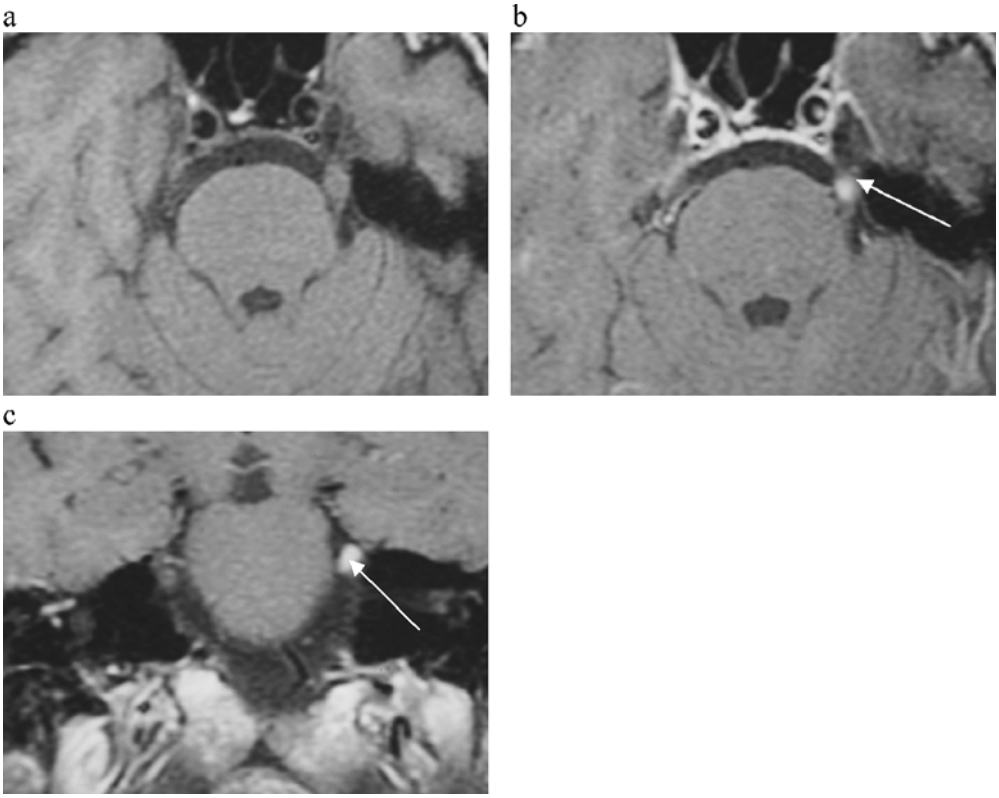

Fig. 5 Trigeminal neuronitis from herpes zoster infection. **a** Axial pre- and (**b**) axial and (**c**) coronal post-gadolinium T1W images through the pons show intense focal enhancement in the cisternal segment of the left trigeminal nerve (white arrows) without significant nerve enlargement (trigeminal neuronitis due to herpes zoster)

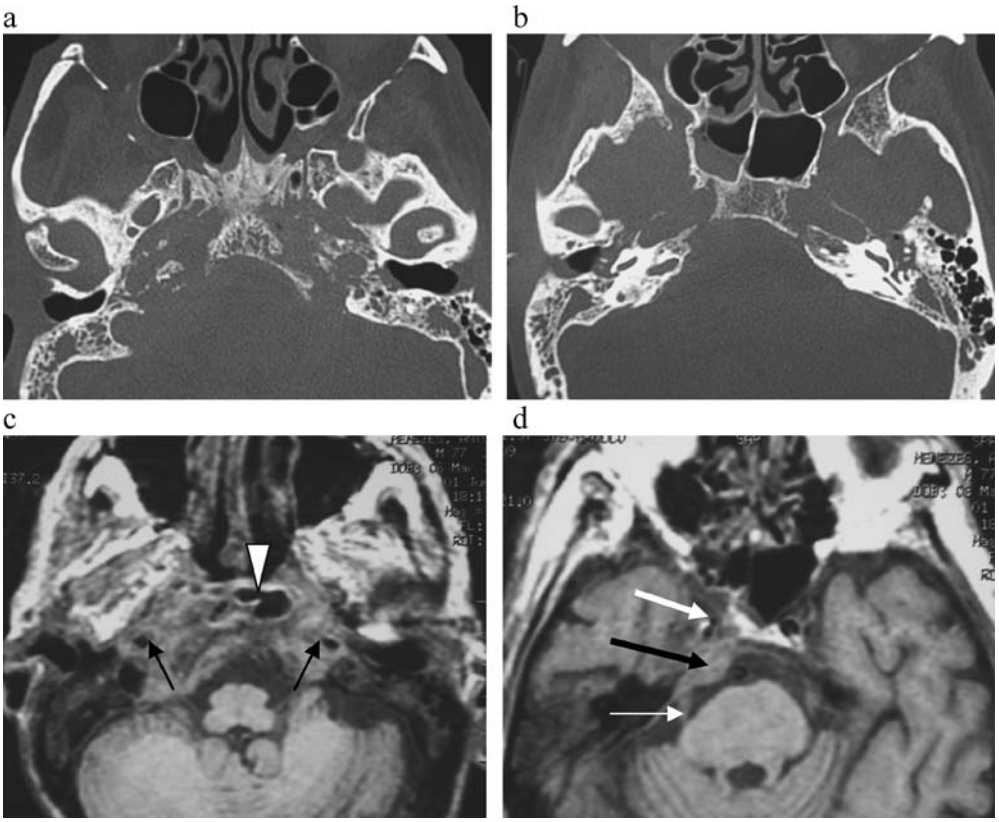

Fig. 6 Skull base osteomyelitis with abscess formation in a diabetic patient presenting with Gradenigo's syndrome. **a** Axial CT (bone algorithm) and (**b**) axial T1W MR images through the central skull base demonstrate a permeative destructive bone pattern involving the central skull base including the clivus, petrous apices and jugular foramen, associated with bilateral opacification of the middle ear cavity and an air-fluid level in the sphenoid sinus. MR shows a soft tissue mass replacing the central skull base, encasing the petrous (thin black arrows) and cavernous internal carotid arteries (thick white arrow), filling in Meckel's cave on the right (thick black arrow) and extending posteriorly along the cisternal segment of the nerve (thin white arrow). Note the presence of a central region of very low T1W signal intensity corresponding to a pocket of fluid (**a**, white arrowhead). (Skull base osteomyelitis with abscess formation in a diabetic patient presenting with Gradenigo's syndrome)

cranial nerves, most often cranial nerves III to VIII, and leading to neural ischemia.

Tuberculous meningitis is the most common form of intracranial tuberculosis, particularly in children. Cranial nerve deficits are a common sequel, most frequently vestibulo-cochlear and oculomotor dysfunction [3]. *Cryptococcal meningitis*, a fungal infection caused by *Cryptococcal neoformans* can be seen in both immunocompetent and immunocompromised patients. The cranial nerve most commonly affected is the optic nerve due to meningeal infiltration around the nerve, chiasm and optic tract, leading to frank ischemia and eventual necrosis [22]. Other fungal infections particularly prone to perineural and perivascular involvement include invasive forms of aspergillosis and mucormycosis, both seen in immunocompromised and diabetic patients [3, 5]. Infection tends to start out in the paranasal sinuses and then spreads into the adjacent soft tissues and intracranial compartment along vessels and nerves and through destruction of the bony walls of the sinus cavities (Figs. 7 and 8). Orbital and cavernous sinus involvement is frequent and courses with cranial nerves I to V deficits. Thrombosis, ischemia and hemorrhagic infarction are common complications. Fungal hypha and mycelia have quite typical imaging features on MR imaging. The presence of metallic ions with paramagnetic effects, most often manganese, is responsible for the low signal intensity on both T1W and T2W images. Henceforth, fungal balls or mycetomas can easily be mistaken for normally aerated sinus on MR imaging [3, 11].

Non-infectious/inflammatory disease processes that may affect the basal meninges and cranial nerves include: sarcoidosis, Wegener's granulomatosis, Behcet disease, inflammatory orbital apicitis (Tolosa-Hunt syndrome), rheumatoid and other connective tissue/immunologic disorders and idiopathic hypertrophic cranial pachymeningitis (Fig. 9) [16]. They all have in common a diffuse or nodular thickening and enhancement of the meninges, with a predilection for the basilar, perimesencephalic and suprasellar regions,

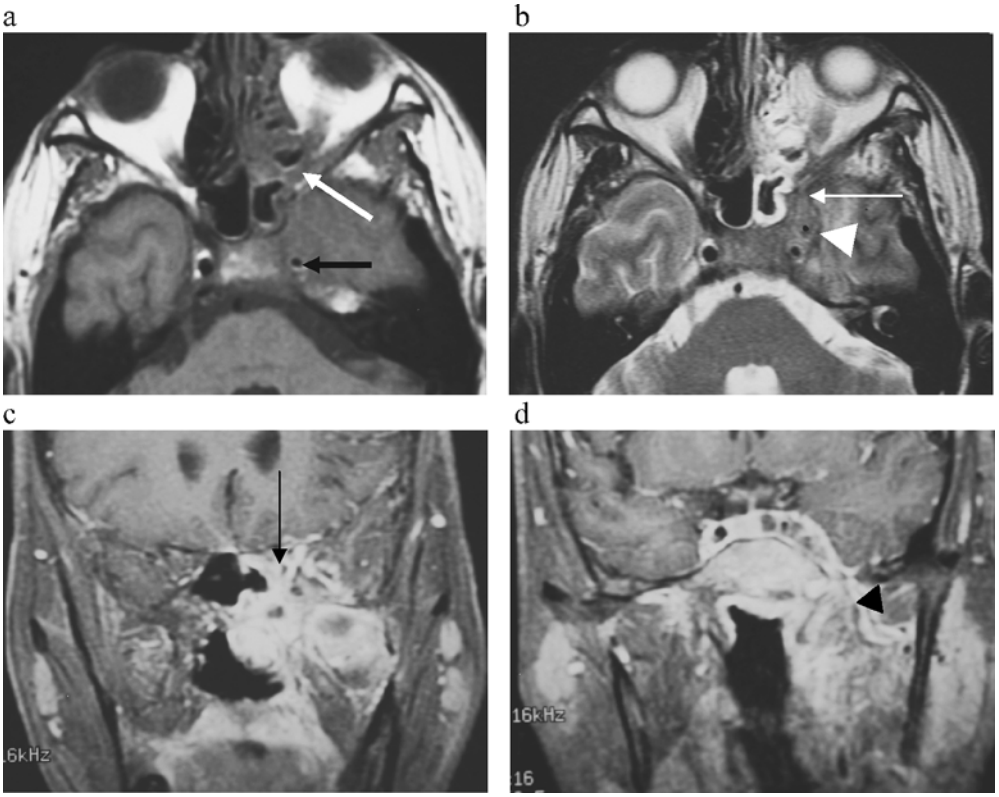

Fig. 7 Invasive mucormycosis in an immunocompromised HIV positive patient. **a** Axial T1W and (**b**) T2W images and coronal contrast-enhanced T1W images through the orbits and paranasal sinuses show heterogenous material filling in the right sphenoethmoidal region, breaching the sinus walls and extending into the inferior orbital fissure (thick white arrow), superior orbital fissure (thin white arrow) and the cavernous sinus (white arrowhead). The soft tissue mass extending intracranially is of low signal intensity on T2W images and encases the cavernous carotid artery, which shows luminal stenosis and irregularity (thick black arrow). The coronal post-gadolinium T1W images (**c** and **d**) show intense enhancement of this mass along with abnormal enhancement of the cavernous segments of cranial nerves III to VI, of the optic nerve at the orbital apex (thin black arrow) and along the course of the mandibular division of the trigeminal nerve (black arrowhead). (Invasive mucormycosis in an immunocompromised HIV positive patient)

Fig. 8 Invasive fungal infection of the sphenoid sinus affecting CN VI. **a** Axial T1W gadolinium-enhanced MR image shows enhancing soft tissue replacing the fatty marrow of the clivus and body of the sphenoid with destruction of the posterior cortical margin (black arrowhead). This abnormal soft tissue extends posteriorly into the pre-pontine cistern involving the basilar plexus and left VIth nerve (black arrow). Note the normal, non-enhancing, contralateral nerve, seen as a grey dot within the bright enhancing plexus (white arrow)

seen on MR imaging with possible involvement of any cranial nerve crossing CSF spaces, resulting in chronic, recurrent cranial neuropathies [3, 5, 16].

Sarcoidosis is a non-necrotizing granulomatous disease that affects the CNS in 16% of cases in autopsy series and 5% of cases in clinical series. Facial nerve involvement is the most common and results from two possible mechanisms: basilar leptomeningitis (Fig. 10) and intraparotid lymphadenopathy [5, 18, 21, 23]. The clinical triad of parotitis, uveitis and bilateral facial nerve paralysis is named Heertfordt syndrome, after the author who first described it.

Wegener's granulomatosis is a non-caseating granulomatous condition that affects the kidneys and respiratory tract. Primary involvement of the sinonasal region is not uncommon and, from there, the inflammatory process may spread intracranially to the frontobasal meninges or into the orbit, affecting most often cranial nerves I and II [3, 22, 24].

In Behcet's disease and rheumatoid arthritis, a meningoencephalitic process is seldom seen, manifesting as abnormal leptomeningeal enhancement. T2W hyperintense enhancing lesions can also be detected deeply around perivascular Virchow-Robin spaces, reflecting angeitis and secondary microvascular ischemic changes [3, 16].

2. Other demyelinating neuropathies
Demyelinating cranial neuropathies can result from inflammation, ischemia, toxic-metabolic or iatrogenic insult such as radiation therapy [16]. Guillain-Barré and Miller-Fisher syndromes may lead to cranial nerve polyneuritis. Diabetes is a common cause of cranial nerve neuropathy. Ischemia and sorbitol deposition in Schwann cells are involved in the pathophysiology of diabetic neuropathy [3]. Among cranial nerves oculomotor nerves (III, IV and VI) are the most commonly affected in diabetic mononeuropathy [3]. Other single cranial nerves may be affected, including the recurrent laryngeal nerve. This neuropathy may be painful and acute in onset and is often reversible over a several week period. Radiation-induced neuropathies are a delayed complication of radiation therapy or radiosurgery [25]. Demyelination, ischemia and coagulation necrosis are the pathologic substrate of this type of injury, resulting in disruption of the blood-nerve barrier with abnormal enlargement and enhancement of the affected nerve(s) [16, 25]. Cranial nerves II and VIII are the most commonly affected. Radiation-induced optic neuritis may ensue years after completion of radiation therapy [22, 25] (Fig. 11). Sensorineural hearing loss is a common complication of radiation therapy to the suprahyoid neck, particularly for nasopharyngeal carcinoma.

3. Trauma
Cranial nerve deficits are a common consequence of trauma, either accidental or iatrogenic secondary to several surgical procedures. There are several factors contributing to cranial nerve susceptibility to trauma: the length, course and vascular supply [26, 27]. The course of the nerve, and, in particular, its relationship with fixed, rigid structures such as bone and dura, largely determine the susceptibility of each individual cranial nerve to trauma as well as the most vulnerable sites to injury [26]. Mechanisms of injury include traction, stretching, impingement and transection of the nerve. Cranial nerve edema and hematoma are usually reversible injuries, whereas nerve disruption requires surgical repair in order to achieve functional recovery [3, 11, 26, 27]. CT is the best imaging modality to assess trauma as it nicely depicts fractures involving the skull base, neurovascular foramina and neural canals. MR is reserved to depict intrinsic neural lesions: neural ischemia and edema resulting in disruption of the blood-nerve barrier manifest as abnormal enhancement; intraneural hematoma may also be depicted with MR by the presence of blood degradation products along the course of the nerve [26, 27]. Complete nerve disruption is not always easy to depict as the neural sheath may remain intact [28].

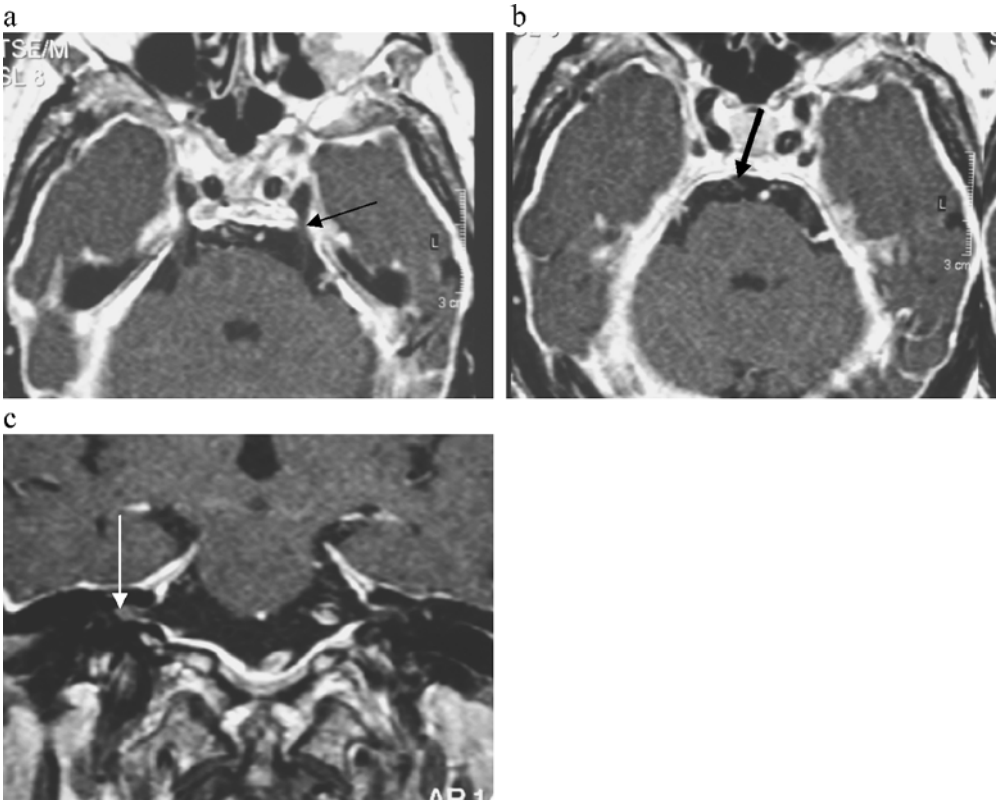

Fig. 9 Idiopathic hyperthrophic pachymeningitis. Axial (**a** and **b**) and coronal (**c**) post-gadolinium T1W images demonstrate diffuse, thick dural enhancement in the posterior fossa and supratentorial compartment. This thick enhancing dura encases the foraminal passages of cranial nerves, namely the porus trigeminus (thin black arrow) and Dorelo's canal (thick black arrow). Also note the abnormal enhancement along the dural covering of cranial nerves VII and VIII (white arrow). (Patient with idiopathic hyperthrophic pachymeningitis)

The facial nerve is commonly injured during blunt head trauma [5, 26]. Injury results from temporal bone fractures, which are present in 5% of cases of craniofacial trauma and constitute the second most common cause of facial nerve paralysis [5, 11, 26]. Longitudinal fractures, the most common, result in facial nerve paralysis in 10% to 20% of cases. The paralysis is often delayed and transient, and results from traction and edema at the level of the geniculate ganglion and proximal tympanic segment. Transverse fractures lead to facial nerve paralysis in 30% to 50% of cases. This paralysis is usually immediate, complete and irreversible. Injury results from impingement and transection of the nerve by a fractured fragment most commonly at the labyrinthine segment, proximal to the geniculate ganglion (Fig. 12) [5, 11, 26, 27].

Anosmia is a frequent complication of blunt head trauma and may result either from frontal or, more often, from occipital blows [24, 26]. The mechanism of injury is thought to be a contracoup shearing effect at the cribiform plate and basal frontal lobes [24]. Imaging may disclose basal frontal lobe contusion involving the gyrus rectus, contusion or avulsion of the olfactory bulbs or fractures of the cribiform plate and nasal vault (Fig. 13) [24].

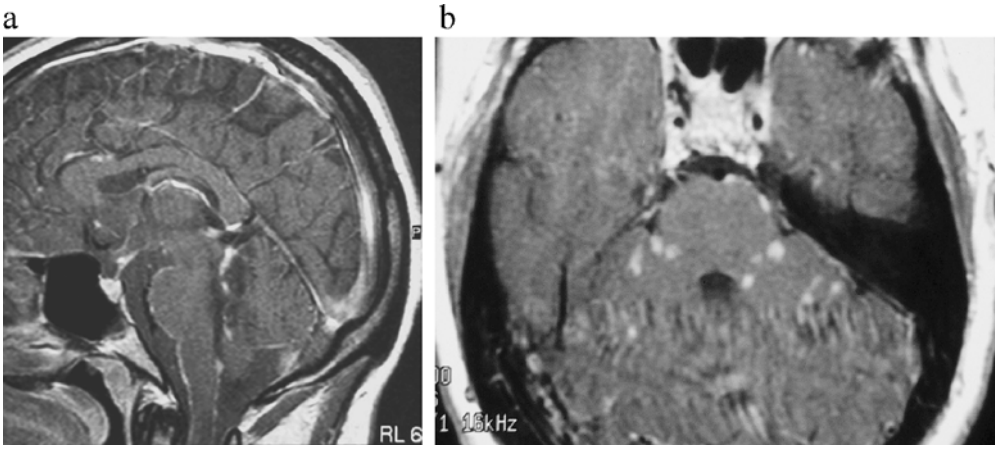

Fig. 10 Neurosarcoidosis. **a** Sagittal and (**b**) axial post-gadolinium T1W images demonstrating thick, irregular and nodular leptomeningeal enhancement, which is more stricking along the basilar and perimesencephalic cisterns, affecting the cisternal segments of the cranial nerves. Note the enhancing nodules along the interpeduncular, crural and pre-pontine cisterns along the course of cranial nerves III, VI, V and VI, respectively

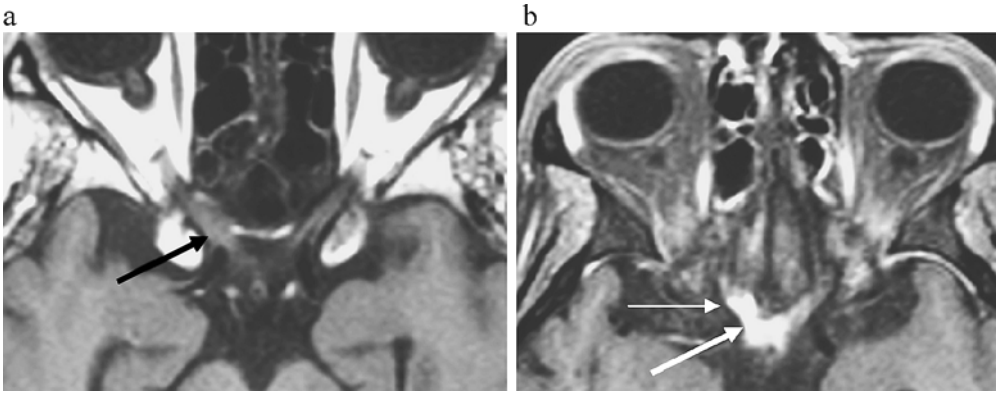

Fig. 11 Radiation necrosis of the optic nerve and chiasm. **a** Axial pre- and post-gadolinium (**b**) T1W images through the orbits demonstrate abnormal enlargement (thick black arrow) and enhancement along the retrocanalicular segments of the optic nerves (thin white arrow) and optic chiasm (thick white arrow), which are more striking on the right. Clinical history was relevant for radiation therapy for nasopharyngeal carcinoma 5 years ago (radiation necrosis)

Post-traumatic injury of the optic nerve is most often associated with orbital and skull base fractures involving the orbital apex or from serious traction of the nerve that, ultimately, results in optic nerve avulsion, most often at its insertion in the back of the globe [22, 28, 29]. The intracanalicular segment is particularly vulnerable due to the close attachment of the dural sheath to the periosteum at the orbital apex and the bony architecture of the orbit that transmits force from the forehead and brow directly to the orbital apex [28, 29]. Imaging may disclose orbital fractures as well as soft tissue thickening or hemorrhage around the insertion of the nerve. Optic nerve contusion and perioptic hemorrhage are best seen on MR [22, 26–29].

Oculomotor deficits are common in the setting of cranio-facial trauma and are probably underestimated as they may be difficult to depict in severely injured patients [30, 31]. Injury may occur at the brain-stem nuclei due to contusion, may result from extreme shearing or nerve avulsion at the root entry zone, or from nerve entrapment secondary to orbital fractures [22, 26, 31]. Gradient echo T2*W images are particularly useful to depict hemorrhagic contusions at the brain-stem exit site of oculomotor nerves [31].

Cranial nerve III is the most frequently damaged. This may result from contusion against the petroclinoid ligament, nerve root tear or complete avulsion at the interpeduncular base [28, 29, 31]. Trauma ranges second or third in the leading causes of oculomotor palsy following vascular lesions and neoplasm in adult series and is the leading cause of acquired third nerve palsy in the pediatric age group [31]. Trauma is the most common cause of isolated trochlear nerve palsy in all age groups and can be uni- or bilateral [26, 29, 31]. The mechanism of injury is usually a contrecoup contusion against the rigid tentorial edge [29, 31]. Because the trochlear nerve decussates at the region of the medullary velum, bilateral injury is not rare [30]. Abducens nerve palsy is the most often recognized oculomotor palsy following trauma in any age group as it leads to a large-angle strabism [26]. Damage results from stretch injury against the rigid clivus in its ascending cisternal segment or from increased intra-

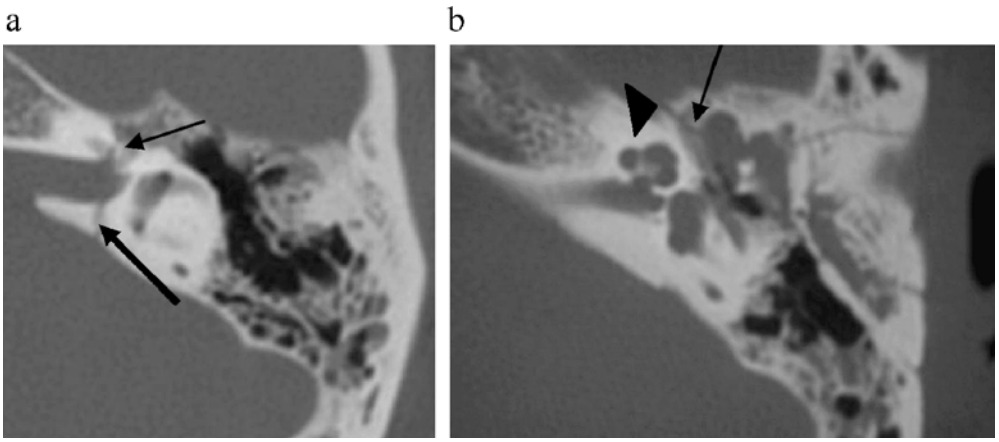

Fig. 12 Fractures of the temporal bone affecting the facial nerve canal. Axial CT images on bone windows. **a** Shows a transverse fracture line through the short axis of the left temporal bone, crossing the internal auditory canal (thick black arrow), the basal turn of the cochlea and the labyrinthine segment of the facial nerve (thin black arrow). **b** Shows an anterior longitudinal fracture through the tympanic segment of the facial nerve (black arrow) and geniculate ganglion (arrowhead). Patients, status post motor vehicle accident, presenting with immediate and complete facial nerve paralysis

Fig. 13 Olfactory bulb contusion. Gadolinium-enhanced coronal T1W image shows a normal non-enhancing olfactory bulb on the left (thick white arrow) and an enhancing right-sided olfactory bulb (thin white arrow) in a patient with post-traumatic hiposmia due to olfactory bulb contusion

cranial pressure. Avulsion against the petrosphenoidal ligament is another possibility [26].

The trigeminal nerve trunk is quite resistant to traumatic injury. This is mainly due to its thickness and short intracranial course. Injury may result from contusion at the porus trigeminus or Meckel's cave [27].

Traumatic injury of the lower cranial nerves (IX to XII) is usually associated with fractures or dislocations affecting the posterior skull base or craniovertebral junction, crossing the jugular foramen, condylar canal or occipital condyles [32]. However, traumatic lesions of the lower cranial nerves are most often iatrogenic.

Iatrogenic injury of cranial nerves occurs during a variety of surgical procedures. To avoid this complication, intra-operative electrophysiologic monitoring of cranial nerves is currently used in high-risk surgeries [5, 11, 18].

Facial nerve paralysis can be a dismal consequence of temporal bone and parotid surgeries. Increased surgical risk results from failure to recognize an abnormal anatomic course or dehiscence of the intratemporal segments of the facial nerve canal before temporal bone surgery and to adequately locate a mass lesion as originating from the parotid gland. The facial nerve can also be injured in neonates during forceps delivery due to its superficial course and incomplete ossification and pneumatization of the mastoid [11, 18, 33].

Lower cranial nerves can be injured during neck dissection, most often the Xth, XIth and XIIth cranial nerves. The inferior loop of the hypoglossal nerve at the submandibular space is often injured during resection of lesions lying in this space [34]. The recurrent laryngeal nerves can be injured during thyroid and parathyroid surgery [32]. However, in most cases, paralysis is usually transient, resulting from hemorrhage and/or edema.

4. Congenital neuropathies

A full description of congenital pathology of cranial nerves is beyond the scope of this article. Although most of these conditions lack adequate treatment, the diagnosis is important to establish the prognosis and to plan functional rehabilitation when possible.

Congenital anosmia and hyposmia are usually associated with choanal atresia, holoprosencephaly, septo-optic dysplasia, sincipital cephaloceles of the fronto-ethmoidal region or Kallmann's syndrome (association of anosmia and hypogonadotrophic hypogonadism). This last condition is often associated with agenesis or hypoplasia of the olfactory bulbs, tracts or olfactory sulci [24].

Septo-optic dysplasia is the most common congenital/developmental lesion of the optic nerve [22, 35]. This condition is characterized by agenesis or hypoplasia of the septum pellucidum and optic nerves and manifests clinically by decreased visual acuity and nystagmus. Due to the high incidence of associated anomalies of neuronal migration including schizencephaly, many authors consider septo-optic dysplasia a mild form of holoprosencaphaly [22, 35]. Hypoplasia of the optic nerves, chiasm and tracts is best appreciated on MR imaging (Fig. 14).

Congenital trigeminal neuropathies have been associated with oculo-auriculo-vertebral dysplasia-hemifacial microsomia (Goldenhar-Gorlin syndrome) [36, 37]. The pathologic substrate of this condition is agenesis of the trigeminal nerve and/or hypoplasia of the trigeminal brain-stem nuclei [36].

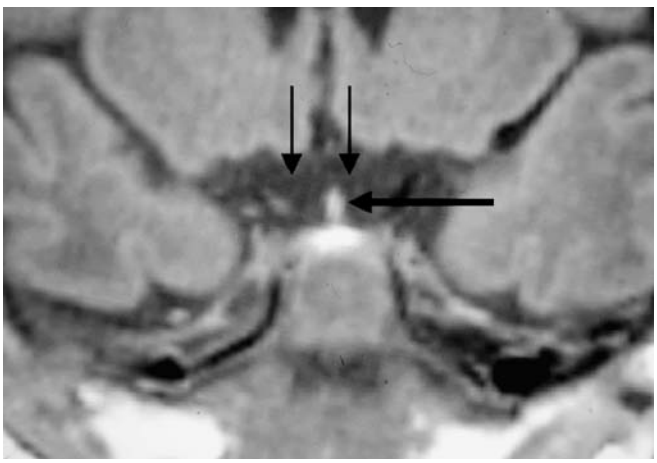

Fig. 14 Septo-optic dysplasia. Coronal T1W image showing absence of the optic chiasm (thin black arrows) and nerves in a neonate with congenital aplasia of the optic nerves, chiasm and eye bulbs. Note the pituitary stalk in its normal position (thick black arrow)

Congenital neuropathies of the facial nerve are often associated with craniofacial malformations involving the 1st and 2nd branchial arches [3, 37]. Uni- and bilateral facial nerve palsy is a feature of Moebius syndrome, a genetic condition characterized by cranial nerve deficits, limb and orofacial anomalies. High-resolution CT scans using bone algorithms are ideal to depict agenesis/hypoplasia of the facial nerve canal and geniculate fossa [9, 10]. Several cranial nerve deficits (from V to XII) have been associated with this syndrome along with MR evidence of ipsilateral brain-stem hypoplasia [36].

There is a wide variety of congenital syndromes (otoskeletal, otocranial-facial and otocervical syndromes) that affect the inner ear and vestibular-cochlear nerve [3, 10]. The most common abnormalities include cochlear and vestibular dysplasia, abnormally enlarged vestibular aqueduct and agenesis or hypoplasia of the vestibular-cochlear nerves [3]. High-resolution sagittal oblique heavily T2W MR images are the gold standard for the diagnosis of agenesis/hypoplasia of the vestibulo-cochlear nerve (Fig. 15) [9, 10].

Cranial neuropathies may also result from nerve compression at the neurovascular foramina in congenital conditions, leading to bone expansion such as fibrous dysplasia, or be secondary to rare congenital hypomyelination neuropathies [33, 36].

Conclusion

Imaging of cranial nerves requires a thorough understanding of neuroanatomy and neurophysiology. Detailed neurologic and electrophysiologic testing can be of great help in the topographic diagnosis, leading to focused imaging studies on specific segments of cranial nerves. High-resolution CT and MR imaging using tailored dedicated protocols has tremendously impacted the diagnostic yield in patients presenting with primary and secondary cranial neuropathies leading to an increasing proportion of recognizable causes of neural dysfunction amenable to specific treatments and functional recovery. Infectious and inflammatory conditions are the most common causes of cranial nerve deficits in the general population and have been increasingly recognized by the use of high-resolution cross-sectional imaging. Traumatic injuries of cranial nerves are frequently underestimated in the acute trauma setting when a detailed neurological evaluation is difficult or impossible to perform and when other life-threatening injuries are a priority. Nonetheless, these injuries should be suspected and recognized as soon

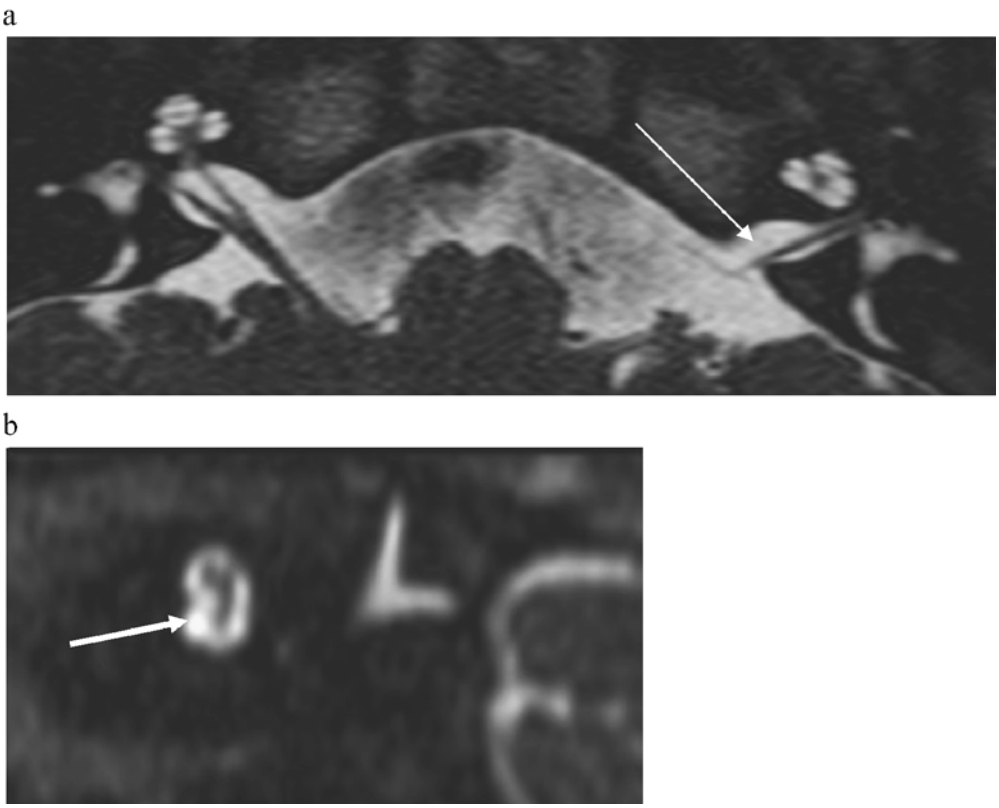

Fig. 15 Agenesis of the vestibulocochlear nerve. **a** Axial and (**b**) sagittal oblique CISS MR image perpendicular to the fundus of the internal auditory canal shows agenesis of the cochlear nerve on the left side (thin white arrow). Note on the sagittal oblique section the facial nerve in the antero-superior quadrant, the vestibular divisions in the posterior quadrant, and the absent cochlear nerve (thick white arrow)

as possible in order to allow early rehabilitation and avoid the troublesome consequences of irreversible cranial nerve deficits. Most congenital neuropathies are, at the present time, beyond medical correction. However, its recognition is mandatory to establish the patient's prognosis and to plan functional rehabilitation whenever possible. In the future, as we move towards higher resolution scanners, further diagnostic improvements are to be expected that will allow evaluation of more peripheral nerve branches and increase the current challenges of cranial nerve imaging.

References

1. Laine FJ, Smoker WR (1998) Anatomy of the cranial nerves. Neuroim Clin N Am 8(1):69–100
2. Wilson-Pawels L, Akeson EJ, Stewart PA (1998) Cranial nerves: anatomy and clinical comments. B. C. Decker Inc, Toronto, Philadephia
3. Som PM, Curtin HD (2003) Head and neck imaging. 4th edn, Mosby, St Louis, MO
4. Leblanc A (2001) Encephalo-peripheral nervous system-Vascularization, anatomy, imaging. Springer, Berlin Heidelberg New York
5. Borges A (2005) Trigeminal neuralgia and facial nerve paralysis. Eur Radiol 15:511–533, March
6. Casselman JW (2006) The upper and lower cranial nerves. Erasmus course on magnetic resonance imaging. Syllabus, Vienna, Austria 13–17 Feb
7. Chavin JM (2003) Cranial neuralgias and headaches associated with cranial vascular disorders. Otolaryngol Clin N Am 36:1079–1093
8. Wichmann W (2004) Reflexions about imaging technique and examination protocol 2. MR examination protocol. Eur J Radiol 49(1):6–7, Jan
9. Stone JA, Chakeres DW, Schmalbrock P (1998) High-resolution MR imaging of the auditory pathway. MRI Clin N Am 6(1):195–219
10. Held P, Fellner C, Fellner F, Seitz J, Graf S, Hilbert M, Strutz J (1997) MRI of the inner ear and facial nerve pathology using 3D MP-RAGE and 3D CISS sequences. Br J Radiol 70 (834):558–566
11. Lufkin RB, Borges A, Villablanca P (2000) Teaching atlas of head and neck imaging, 1st edn. Thieme, New York, Stuttgart
12. Lufkin RB, Borges A, Nguyen K, Anzai Y (2001) MRI of the head and neck, 2nd edn. Lippincott Williams & Wilkins, Philadelphia
13. Jager L, Reiser M (2001) CT and MR imaging of the normal and pathologic conditions of the facial nerve. Eur J Radiol 40(2):133–146
14. Majoie CB, Hulsmans FJ, Verbeeten B et al (1997) Trigeminal neuralgia: comparison of two MR imaging techniques in the demonstration of neurovascular contact. Radiology 204:455–460
15. Yoshino N, Akimoto H, Yamada Y, Nagaoka T, Tetsumura A et al (2003) Trigeminal neuralgia: evaluation of neuralgic manifestation and site of neurovascular compression with 3D CISS MR imaging and MR angiography. Radiology 228(2):539–545
16. Saremi F, Helmy M, Farzin S, Zee CS, Go JL (2005) MRI of cranial nerve enhancement. AJR Am J Roentgenol 185(6):1487–1497, Dec
17. Suzuki F, Furuta Y, Ohtani F, Fukuda F, Inuyama Y (2001) Herpes virus reactivation and gadolinium enhanced magnetic resonance imaging in patients with facial palsy. Otol Neurotol 22 (4):549–553
18. Philips CD, Bubash LA (2002) The facial nerve: anatomy and common pathology. Semin Ultrasound CT MR 23(3):202–217
19. De Marco JK, Hesselink JR (1993) Trigeminal neuropathy. Neuroimaging Clin N Am 3:117
20. Johnston JL (2002) Parasellar syndromes. Curr Neurol Neurosci Rep 2:423–431
21. Roob G, Fazekas F, Hartung HP (1999) Peripheral facial palsy: etiology, diagnosis and treatment. Eur Neurol 41:3–9
22. Smith MM, Strottmann JM (2001) Imaging of the optic nerve and visual pathways. Semin Ultrasound CT MR 22(6):473–487, Dec
23. Benecke JE (2002) Facial paralysis. Otolaryngol Clin N Am 35(2):357–365
24. Yousem DM, Oguz KK, Li C (2001) Imaging of the olfactory system. Semin Ultrasound CT MR 22(6):456–472, Dec
25. Pradat PF, Poisson M, Delattre JY (1994) Radiation-induced neuropathies. Experimental and clinical data. Rev Neurol (Paris) 150(10):664–677, Oct
26. Hanson RA, Gosh S, Gonzalez-Gomez I, Levy ML, Gilles FH (2004) Abducens length and vulnerability? Neurology 13(62):33–36, Jan
27. Mariak Z, Mariak Z, Stankiewicz A (1997) Cranial nerve II-VII injuries in fatal closed head trauma. Eur J Opthtalmol 7(1):68–72, Jan-Mar
28. Mcann JD, Steiff S (1994) Traumatic neuropathies of the optic nerve, optic chiasm, and ocular motor nerves. Curr Opin Ophthalmol 5(6):3–10
29. Lagreze WA (1998) Neuro-ophthalomology of trauma. Curr Opin Ophthalmol 9(6):33–39, Dec
30. Majoie C (2002) Magnetic resonance imaging of the brainstem and cranial nerves III to VII. Mov Disord 17(2): S17–S19
31. Balcer LJ, Galeta SL, Bagley LJ, Pakola SJ (1996) Localization of traumatic oculomotor nerve palsy to the midbrain exit site by magnetic resonance imaging. Am J Ophthalmol 122 (3):437–439, Sept
32. Larson TC 3rd, Aulino JM, Laine FJ (2002) Imaging the glossopharyngeal, vagus and accessory nerves. Semin Ultrasound CT MR 23(3):238–255, Jun
33. Carr MM, Ross DA, Zucker RM (1997) Cranial nerve defects in congenital facial palsy. J Otolaryngol Apr 26 (2):80–87
34. Loh C, Maya MM, Go JL (2002) Cranial nerve XII: the hypoglossal nerve. Semin ultrasound CT MR 23 (3):256–265, Jun
35. Egan RA, Kerrison JB(2003) Survey of genetic neuro-ophthalmic disorders. Opthalmol Clin North Am 16(4):595–605, Dec
36. Allen BM, Wert MA, Tatum SA (2006) Congenital unilateral multiple cranial neuropathy: an etiology shared with Mobius syndrome? Int J Pediatr Otorhinolaryngol 70(5):931–934, May
37. Aleksi S, Budzilovich G, Reuben R, Feigin I, Finegold M, McCartthy J et al (1975) Congenital trigeminal neuropathy in oculoauriculovertebral dysplasia-hemifacial microsomia (Goldenhar-Gorlin syndrome). J Neurol Neurosurg Psychiatry 38(10):1033–1035, Oct